

ACOUSTIC INDICES OF CARDIAC FUNCTIONALITY

Guy Amit¹, Jonathan Lessick^{2,3},

¹*School of Computer Science, Tel-Aviv University, Tel-Aviv, Israel*

²*Department of Cardiology, Rambam Medical Center, Haifa, Israel*
gamit@tau.ac.il, j_lessick@rambam.health.gov.il

Noam Gavriely³, Nathan Intrator¹

³*Rappaport Faculty of Medicine, Technion-Israel Institute of Technology, Haifa, Israel*
gavriely@tx.technion.ac.il, nin@tau.ac.il

Keywords: Heart sounds, time-frequency analysis, feature extraction, cardiac functionality

Abstract: The mechanical processes of the cardiac cycle generate vibratory and acoustic signals that are received on the chest wall. We describe signal processing and feature extraction methods utilizing these signals for continuous non-invasive monitoring of cardiac systolic function. Vibro-acoustic heart signals were acquired from eleven subjects during a routine pharmacological stress echocardiography test. Principal component analysis, applied to the joint time-frequency distribution of the first heart sound (S1), revealed a pattern of an increase in the spectral energy and the frequency bandwidth of the signal associated with the increase of cardiac contractility during the stress test. Novel acoustic indices of S1 that compactly describe this pattern showed good linear correlation with reference indices of systolic functionality estimated by strain-echocardiography. The acoustic indices may therefore be used to improve monitoring and diagnosis of cardiac systolic dysfunctions.

1 INTRODUCTION

The human heart is a mechanical system whose primary function is to pump blood throughout the body in order to provide adequate perfusion of organs. This function is achieved by a complex interplay between the cardiac muscle, the vascular system and the blood, highly regulated by mechanical and neural control mechanisms. Cardiovascular diseases, such as coronary artery disease, hypertension and cardiomyopathy, may impair the mechanical functionality of the heart, leading to the clinical syndrome of heart failure (HF). As these diseases are major public health problems worldwide, technologies for improving early diagnosis and patient monitoring are essential.

The low-frequency vibratory and acoustic signals, produced by the mechanical processes of the cardiac cycle and received on the chest wall, provide a direct and simple way for assessing the mechanical functionality of the cardiovascular system (Tavel, 1978). However, the utilization of these signals in the clinical setting has been mostly limited to

qualitative assessment by manual methods, as research and development efforts in recent years focused on modern imaging technologies such as echocardiography and cardiac computerized tomography. These valuable techniques require complex equipment, as well as expert operators and interpreters. In particular, these imaging tools can not be used continuously or outside of the hospital environment. Consequently, long-term non-invasive monitoring of mechanical functionality remains unavailable in the common medical practice.

In this work, we revisit the problem of quantitative analysis of mechanical vibro-acoustic heart signals using modern signal processing tools. In an earlier study, we have shown the feasibility of using vibro-acoustic signals to extract temporal information about the phases of the cardiac cycle (Amit, 2005). In the current study, we address the potential of continuously assessing the global systolic functionality of the left ventricle using indices extracted from the first heart sound, S1. According to Rushmer's theory of the origin of heart sounds, S1 is generated by the vibrations of the

entire cardiohemic system, as a result of blood acceleration and deceleration following the onset of ventricular contraction and the closure of the atrioventricular valves (Rushmer, 1978). The amplitude of S1 has been previously shown to be related to the pressure gradient (dP/dt) developing in the left ventricle during isovolumetric contraction (Sakamoto, 1965). A good correlation was also reported between dP/dt and the instantaneous frequency of S1 (Chen, 1997). While these previous studies were performed on anesthetized dogs, the relation between the characteristics of S1 and global left-ventricular systolic functionality has not been studied in humans in routine clinical settings.

We study the relationship between acoustic indices, extracted from the time-frequency energy distribution of S1, and reference echocardiographic indices that are related to left-ventricular systolic functionality. To achieve dynamic, yet controllable, hemodynamic conditions, we used clinical settings of a routine echocardiography pharmacological stress test. In the following sections, we describe the signal processing and feature extraction methods applied to the vibro-acoustic heart signal, introduce novel acoustic indices of systolic functionality and present quantitative results on the correlation between these indices and echocardiography-derived measures. We conclude by discussing the potential applicability of our methods for continuous non-invasive monitoring of cardiac systolic function.

2 METHODS

2.1 Patients and Protocol

The study was approved by the local ethics committee for medical research. Data was acquired from eleven male subjects of ages 36-79 (mean 60 ± 14), referred to a routine Dobutamine stress echo test (DSE) for assessment of ischemic heart disease. The referral indications included positive ergometry stress test, atypical chest pain and chest pain during physical activity. Two of the subjects had a history of coronary artery disease. These two subjects were diagnosed as positive for myocardial ischemia in the DSE test. The remaining nine patients were diagnosed as negative for ischemic heart disease. Prior to data recording, the patients signed an informed consent form. The standard DSE protocol consisted of four 3-minute stages of increasing Dobutamine dosage, from 10 to $40 \mu\text{g}/\text{kg}/\text{min}$. If the target heart rate, defined as $0.85 * (220 - \text{Age})$, was not achieved at the end of the final stage, 0.25 mg

boluses of atropine were given at 1-min intervals, up to a maximum of 1 mg.

2.2 Data Acquisition

Vibro-acoustic heart signals were recorded using a digital data acquisition system constructed in our lab. The system consisted of 4 piezoelectric contact transducers (PPG Sensor Model 3, OHK Medical Devices, Haifa, Israel), an ECG sensor (EKG-BTA, Vernier Software & Technology, Beaverton, OR), a preamplifier with high input impedance and a linear frequency range of 1Hz – 4KHz (A.S. ZLIL, Bnei-Brak, Israel), a 16-bit analog-to-digital converter (PMD-1608FS, Measurement Computing Corp., Norton, MA), and a designated signal recording software running on a portable personal computer.

The transducers were placed at the apex area, the aortic and pulmonary areas (second intercostal space, right and left sternal border, respectively) and at the right carotid artery, and were firmly attached using either elastic straps or adhesive bands. The patients were lying on their left side. Vibro-acoustic and ECG signals were continuously recorded during the stress test (30-45 minutes long) at a sample rate of 4KHz. Echocardiography images were acquired using a GE Vivid 7 ultrasound machine (General Electric Healthcare, Wauwatosa, WI). Two-dimensional echo cine loops of a single heart beat were captured before the beginning of the stress test (baseline), during each stage of the test and following the test (recovery), from three apical views (4-chamber, 2-chamber and apical long axis) at a high frame rate of 70-100 FPS.

2.3 Echo Data Processing

The captured echo cine loops were post-processed using EchoPAC Dimension '06 software (GE Healthcare Wauwatosa, WI) in order to extract quantitative echocardiographic indices of systolic functionality. The indices used were peak systolic velocity (PSV) and peak systolic strain rate (PSSR), shown to be strongly correlated with left-ventricular systolic functionality (Greenberg, 2002). These indices were first calculated separately for each cardiac wall (septal, lateral, inferior, anterior, posterior, and anteroseptal) and for three segments per wall (basal, middle and apical), and then averaged to obtain a global functionality index. Index calculation was done using 2D strain analysis, based on speckle tracking technique. This modality allows objective analysis of the entire myocardial motion throughout the heart cycle by tracking

natural acoustic markers in the image. It was shown to provide accurate strain measurements, compared with tagged MRI (Amundsen, 2006). Strain indices were successfully calculated for 10 patients. One patient was excluded due to inadequate quality of the captured echo images.

2.4 Acoustic Signal Processing

Each of the four recorded signal channels was first pre-processed by applying a digital band-pass filter in the frequency range of 20-250Hz (Figure 1a). The signal was then partitioned into cardiac cycles using the peaks of the ECG-QRS complexes as reference points (Figure 1b). Signal segments with noisy ECG were excluded from the analysis. The signal cycles were aligned by their starting points and their amplitudes were color-coded to create a two-dimensional signal map, showing the time-domain dynamics of the first and second heart sounds throughout the stress test (Figure 1c). Fast Fourier transform (FFT) was applied to each cycle of the first heart sound (S1), defined as the cycle segment from 50ms before the QRS peak to 200ms after the QRS peak. The logarithm of the power spectrum was color-coded to generate a spectral map of S1 throughout the recording (Figure 1d).

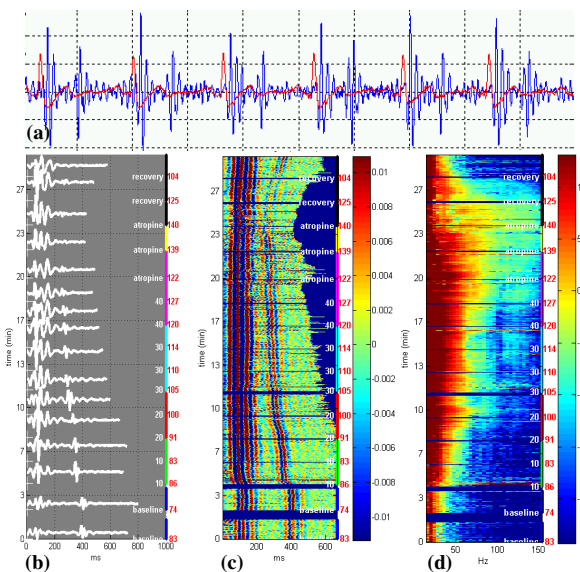


Figure 1: Generation of time-domain and frequency-domain signal maps in a healthy subject: (a) the heart sound signal (blue), segmented using the ECG (red). (b) aligned multiple sound signal cycles throughout the test (left y-axis), with heart rate (red labels) and test staged (white labels and colored segments), (c) continuous color-coded map of segmented sound signals (d) continuous color-coded power spectrum of the first heart sound (S1).

In order to characterize the joint time-frequency energy distribution of S1, S-transform was applied to each cycle of S1. S-transform (Stockwell, 1996) is a linear transform that provides frequency-dependent resolution, while maintaining a direct relationship with the Fourier spectrum. It is defined by:

$$S(\tau, f) = \int_{\mathcal{R}} s(t) \frac{|f|}{\sqrt{2\pi}} e^{-\frac{(\tau-t)^2 f^2}{2}} e^{-i2\pi f t} dt$$

Where $s(t)$ is the original signal, τ is the time delay and f is the frequency. The progressive resolution of the transform provides a time-frequency resolution superior to Fourier-based techniques, while its linearity ensures accurate decomposition without artifactual cross-terms that are typical to quadratic transforms. S-transform is therefore suitable for analysis of non-stationary multi-component signals such as heart sounds.

After applying S-transform to each cycle of S1, the resulting time-frequency representations were grouped by the stages of the stress test and averaged to produce a small number of representative time-frequency maps (Figure 2).

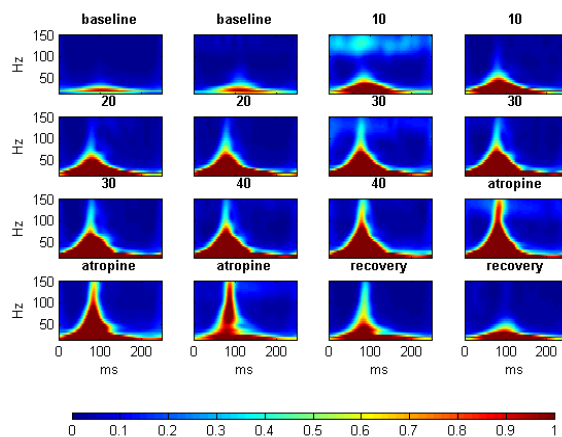


Figure 2: S-transform time-frequency representation of S1 acoustic signal obtained in a representative healthy subject during the stages of the stress test. Each plot represents an average of the S-transform of all S1 cycles over a specified period of the test.

2.5 Acoustic Feature Extraction

The purpose of feature extraction is to find a compact representation of high dimensional data, without significant loss of information content. Principal component analysis (PCA) is a well-known statistical technique for dimensionality reduction (Duda, 1973). The principle of PCA is to

project the data on a new orthogonal basis, such that the variances of the linearly transformed data are sorted in descending order along the coordinates, with the maximal variance on the first coordinate (first principle component), the second largest variance on the second coordinate, and so on. The projection of the original data on the first few principal components provides a low-dimensional representation of the data, which emphasizes the significant features (in terms of statistical variability) in the data. The choice of the significant principal components is done by examining their associated eigenvalues.

PCA was applied on the aggregation of segmented S1 signals. The analysis was performed on both the frequency domain spectral maps (Figure 1d) and on the time-frequency representations produced by the S-transform (Figure 2), vectorized by concatenating adjacent columns. The most significant principal components, having eigenvalues greater than 10% of the first eigenvalue, were selected and weighted by their relative eigenvalues. The projection of the data on this weighted combination of the significant principal components was chosen as a one-dimensional feature representing the dynamic characteristics of the acoustic signal during the stress test. To obtain an interpretable trend line, this feature was normalized by the median value of the baseline stage and smoothed by a moving average filter. The resulting index, denoted acoustic variability index (AVI) is interpreted as the trend of relative change in the spectral energy distribution of S1.

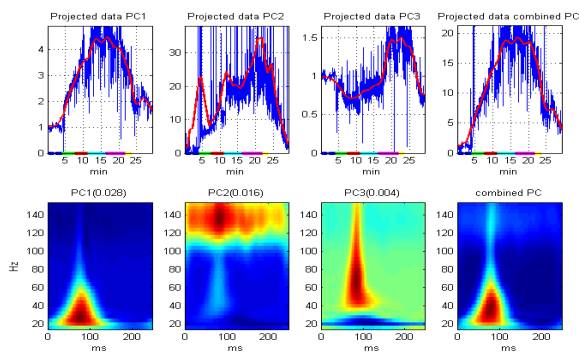


Figure 3: Principal component analysis applied to the vectorized time-frequency representation of S1 cycles during a stress test. The bottom plots show the coefficients of the first 3 principal components (PC), and their linear combination, weighted by the eigenvalues (shown in parenthesis). The upper plots show the AVI index during the entire stress test, obtained by projecting the data on the respective PC. The red lines are the result of smoothing the projected data with a moving-average filter.

Figure 3 illustrates an example of applying PCA to the time-frequency data shown in Figure 2, and calculating the time-frequency AVI.

A second feature extracted from the spectrum of each cycle of S1 was the frequency bandwidth of the signal, defined by the highest frequency with significant energy content. Prior to calculating this feature, signal cycles with a high wide-band energy content, compared to their local environment, were classified as noise and excluded from further processing. The bandwidth feature was calculated for each cycle by searching the spectrum for the first frequency whose energy is at least 10dB below the maximal energy. The feature trend line obtained from all cycles was normalized by the median value of the baseline stage, and denoted Acoustic Spectral Index (ASI).

3 RESULTS

The color-coded signal map in Figure 1c illustrates the time-domain characteristics of the heart sound signal during the stress test. As expected, there are noticeable changes in the duration of ventricular systole and diastole, as the heart rate increases in exercise and decreases in recovery. However, there are no apparent morphological changes in the signal that can be associated with the stress response. Fourier analysis uncovers a pattern of an ascent in the spectral energy of the first heart sound as the Dobutamine dose is increased, and a descent back to baseline levels during recovery (Figure 1d). In addition to the overall energy rise, there is also an increase in the frequency bandwidth of S1, as higher frequency components in the range of 50-150Hz emerge and strengthen. The time-frequency representation, obtained by S-transform, enables localization of these spectral changes in time (Figure 2): the high-frequency components are centered about 80ms after the beginning of the signal (30ms after the peak of ECG-QRS complex), growing up to 150Hz in the highest Dobutamine dose, then falling back to the baseline upper-limit frequency of 50Hz in the recovery phase. There is no apparent time shift of the signal's energy distribution throughout the test.

Principal component analysis, applied to the spectral maps of S1, was able to identify the major frequency bands that contribute to the data variability. When applied to the vectorized time-frequency distributions, PCA also pointed out the temporal location of these frequency bands. Figure 3 shows a representative example of the coefficients of

the first three principal components (PC), and the projection of the time-frequency data on these principal components. The first PC, representing the axis with the largest data variability, captures the pattern already observed qualitatively in the time-frequency distributions in Figure 2: it varies from 30ms to 120ms relative to the beginning of the cycle, and from frequency of 20Hz to 70Hz, thus showing the strengthening of the signal's low-frequency components. The second PC captures the variability of the high frequency components between 110 to 150Hz for the entire duration of the S1 signal. The third PC shows a wide-band variability of frequency ranging from 40Hz to 150Hz, localized in time around 80ms from the beginning of the cycle. This component strengthens during the peak stress response. A combination of the most significant principal components, weighted by their eigenvalues, and the projection of the data on this combined PC provide a one-dimensional feature, denoted time-frequency acoustic variability index (TF-AVI), which summarizes the dynamics of the joint time-frequency energy distribution of S1 throughout the stress test.

The TF-AVI trend lines, extracted separately from each of the four transducers in two representative subjects are plotted in Figure 4, along with the stages of the stress test, the heart rate and blood pressure trends and the relative change in the echocardiographic indices of peak systolic velocity (PSV) and peak systolic strain rate (PSSR). While the TF-AVI provides a continuous line with one point per cardiac cycle, the reference echocardiographic indices are available only at discrete time points of each stage in the stress test. Nevertheless, there is a noticeable correlation between the two indices: for the plot in Figure 4a (subject #5), the correlation coefficients between the echo indices PSV and PSSR and the corresponding TF-AVI, averaged over all transducers were 0.91 and 0.89 respectively. For the plot in Figure 4b (subject #6) the correlation coefficients were 0.97 and 0.83 ($p < 0.05$ in all cases).

Both paired and unpaired t-test showed that the absolute values of the acoustic spectral index (ASI) at the end of low-dose Dobutamine induction were significantly higher than the baseline values ($p < 0.04$ for the 10ug stage, $p < 0.003$ for the 20ug stage, Figure 5). The correspondence between the ASI and the echocardiographic indices in all of the subjects was tested by comparing the values of the relative index change at the end of the low-dose Dobutamine stages. These points were selected since the inotropic effect is more prominent at the early stages

of the test. In addition, the higher heart rates at later stages of the test reduce the reliability of the tissue tracking procedure used to extract the reference echocardiographic indices. As shown in Figure 6, a good linear correlation ($r = 0.78$, $p < 0.01$) was observed between ASI calculated from the apex signal and the relative PSSR at the end of the 20ug stage. At the end of the 10ug stage the correlation coefficient between the two indices was 0.68 ($p < 0.03$).

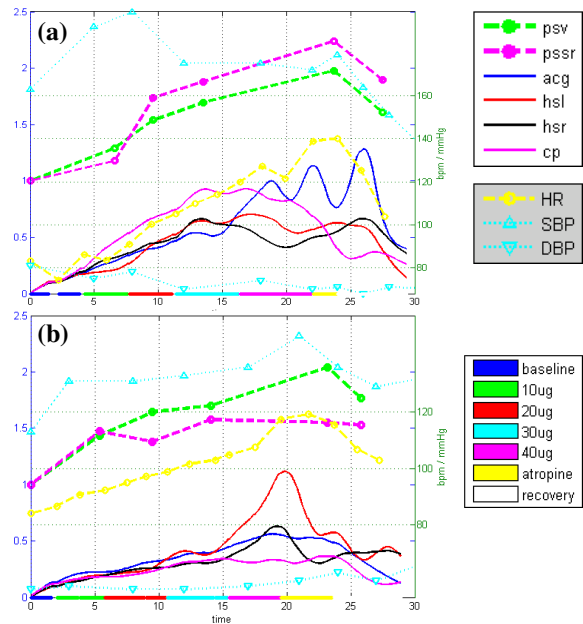


Figure 4: TF-AVI indices of subjects #5 (a) and #6 (b). Each plot displays the trend lines of TF-AVI from the transducers at the apex (acg), aortic area (hsr), pulmonary area (hsl) and carotid artery (cp), along with the relative echo indices PSV and PSSR, trend lines of heart rate and blood pressure, and color-coded stages of the stress test. See text for details.

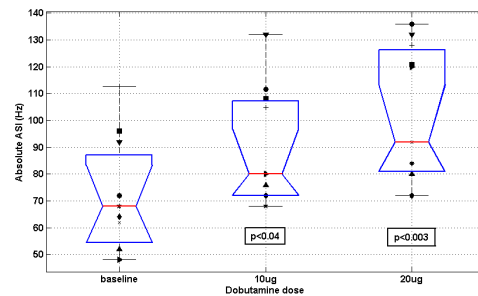


Figure 5: Absolute ASI values of all subjects at baseline and after low-dose Dobutamine induction (10 and 20 ug/kg/min). The box plot displays the median, lower quartile, upper quartile and data extent. Each marker symbol represents a different subject. The p-values represent a t-test comparison to the baseline values.

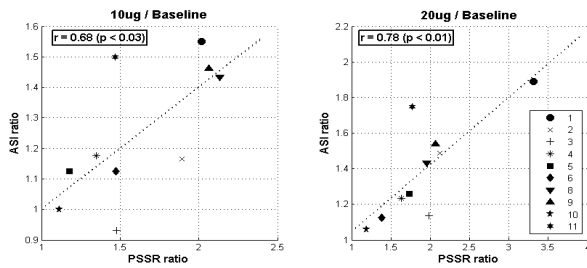


Figure 6: The correlation and regression line between relative PSSR index and relative ASI at the end of first (10ug) and second (20ug) low-dose Dobutamine induction. Each marker symbol represents a different subject.

4 DISCUSSION

More than 40 years ago, Sakamoto et al. reported a nearly linear relationship between the amplitude of the first heart sound, S1, and the maximum of the time derivative of the left ventricular systolic pressure (dP/dt) in dogs (Sakamoto, 1965). Later it was shown that myocardial infarction in humans caused a shift of the maximum energy of S1 to a lower frequency range (Adolph, 1970), and that a reduction in the spectral energy of S1 correlated well with the presence of significant coronary artery disease (Clarke, 1978). More recently, Chen et al. showed a good cross-correlation between the instantaneous frequency of S1 and dP/dt of dogs in various contractile states (Chen, 1997). They suggested that the resonant frequency of S1 is proportional to the fractional power of the tension of the left-ventricular myocardium during contraction, which relates to the left ventricular pressure gradient by Laplace's law. The results of the current study are in agreement with these previous studies regarding the relation between the amplitude and frequency spectrum of the first heart sound and the dynamics of left ventricular contraction. The acoustic indices developed in the current study exhibited a marked correlation with the pattern of inotropic and chronotropic changes throughout the Dobutamine stress test. The increase in the spectral energy, along with the emergence of higher frequency components was consistently observed in multiple recording locations in all of the subjects. Although the study was conducted on a small group of subjects, statistically significant differences were observed across-subjects between baseline and low-dose Dobutamine stages, confirming the reliability of the results. The good correlation obtained with the reference strain echocardiography indices suggests

that the acoustic indices truly characterize the variations in the myocardial systolic functionality. The relationship between the cardiovascular physiological processes and their acoustic manifestation on the chest wall is complex and most probably non-linear. This relationship is affected by neurohormonal modulation of the heart's inotropic and chronotropic states, as well as by changes in the properties of the thoracic cavity conducting the acoustic vibrations. Nevertheless, this work provides a framework and a set of computational tools for robust quantitative analysis of vibro-acoustic heart signals that can be utilized for non-invasive, continuous monitoring of cardiac functionality.

The capability of this framework to diagnose a pathologic functionality reduction could not be addressed quantitatively in this work, due to the small number of subjects and the fact that the great majority of the subjects had normal cardiac functionality. Interestingly, the single subject that was diagnosed in the echocardiography examination with a reduced segmental wall motion during stress, due to myocardial ischemia (subject #10) had the lowest values of absolute and relative ASI, as well as the lowest values of PSSR, indicating that the compromised wall motion might result in a frequency reduction of the first heart sound.

The usage of strain-echocardiography indices for evaluation of left-ventricular function is still not a part of the common clinical practice. Nevertheless, there are strong research evidences for the relation between peak strain rate and the invasive contractility measure of peak elastance (Greenberg, 2002), and for the ability of global strain indices to detect left-ventricular systolic dysfunction. (Reisner, 2004). Strain echocardiography was therefore used in this research as a quantitative 'gold-standard' reference, which can be obtained non-invasively during the routine protocol of the stress test.

One of the major challenges of extracting meaningful physiological information from signals acquired in routine clinical settings is noise robustness. The data used in this work was contaminated with various types of noise, including body movements, interferences of the ultrasonic transducer and audible sounds. The signal analysis methods used in this work were specifically designed to cope with these types of noise. In particular, the statistical approach of transforming the data to a new orthogonal basis of the principal components was able to accentuate physiologically meaningful patterns, while diminishing noisy-related components.

5 CONCLUSIONS

We have described a signal analysis framework for robust extraction of systolic functionality indices from acoustic heart signals. The developed tools were constructed and tested on data from a pharmacological stress test, with strain echocardiography as the gold standard reference. Using principal component analysis on the time-frequency representation of the first heart sound we have characterized the pattern of spectral changes occurring during the stress test, and associated this pattern to the alternations in systolic functionality by showing it is linearly correlated to echocardiography derived indices of cardiac contractility. Our analysis framework and proposed indices can be applied to real-time continuous monitoring of cardiac functionality, thus enabling improved diagnosis and management of cardiac dysfunction.

ACKNOWLEDGEMENTS

We would like to express our gratitude to the team of the Echocardiography lab at the Rambam medical center, for their kind assistance in data collection.

We would like to thank Dr. Zvi Friedman and Dr. Peter Lysyansky from GE Healthcare for providing the strain echocardiography analysis tools.

REFERENCES

- Adolph, R.J., Stephens, J.F., Tanaka, K., 1970. The clinical value of frequency analysis of the first heart sound in myocardial infarction, *Circulation* 41:1003-1014.
- Amit, G., Gavriely, N., Lessick, J., Intrator, N., 2005. Automatic Extraction of Physiological Features from Vibro-Acoustic Heart Signals: Correlation with Echo-Doppler, *Computers in Cardiology* 2005:299-302.
- Amundsen, B.H., Helle-Valle, T., Edvardsen, T., Torp, H., Crosby, J., Lyseggen, E., Støylen, A., Ihlen, H., Lima, J.A.C., Smiseth, O.A., Sjørdahl, S.A., 2006. Noninvasive Myocardial Strain Measurement by Speckle Tracking Echocardiography, *J Am Coll Cardiol*, 47:789-793.
- Chen, D., Durand, L.G., Lee, H.C., Wieting, D.W., 1997. Time-frequency analysis of the first heart sound: Part 3, *Med. Biol. Eng. Comput.* 35:455-461.
- Clarke, W.B., Austin, S.M., Pravib, M.S., Griffen, P.M., Dove, J.T., McCullough, J., Schreiner, B.F., 1978. Spectral Energy of the First Heart Sound in Acute Myocardial Ischemia, *Circulation* 57:593-598.
- Duda, R.O., Hart, P.E., 1973. *Pattern Classification and Scene Analysis*. Wiley New-York.
- Greenberg, N.L., Firstenberg, M.S., Castro, P.L., Main, M., Travaglini, A., Odabshian, J.A., Drinko, J.K., Rodriguez, L.L., Thomas, J.D., Garcia, M.J., 2002. Doppler-Derived Myocardial Systolic Strain Rate Is a Strong Index of Left Ventricular Contractility, *Circulation* 105:99-105.
- Reisner, S.A., Lysyansky, P., Agmon, Y., Mutlak, D., Lessick, J., Friedman, Z., 2004. Global Longitudinal Strain: A Novel Index of Left Ventricular Systolic Function, *J Am Soc Echocardiogr* 17:630-633.
- Rushmer, R.F., 1978. *Cardiovascular Dynamics*, WB Saunders Co. Philadelphia, 4th edition.
- Sakamoto, T., Kusukawa, R., MacCanon, D.M., Luisada A.A., 1965. Hemodynamic Determinants of the Amplitude of the First Heart Sound, *Circ. Res.* 16:45-57.
- Stockwell, R., Mansinha, L., Lowe, R., 1996. Localization of the complex spectrum: the S transform, *IEEE Transactions on Signal Processing*, 44:998-1001
- Tavel, M.E., 1978. *Clinical Phonocardiography & External Pulse Recording*. Year Book Medical Publishers Inc. Chicago, 3rd edition.